applied sciences

MDPI

Article

Mechanical Behaviour of HDPE Agricultural Nets Under Accelerated Aging: Experimental Tensile and Structural Analysis

Roberto Puglisi [1,*], Greta Mastronardi [2], Audrey Maria Noemi Martellotta [3], Sergio Castellano [4], Giuseppe Starace [5], Ileana Blanco [2], Giacomo Scarascia Mugnozza [3] and Pietro Picuno [1,*]

[1] Department of Agricultural, Forest, Food, and Environmental Sciences (DAFE), University of Basilicata, Via dell'Ateneo Lucano, n.10, 85100 Potenza, PZ, Italy
[2] Department of Biological and Environmental Sciences and Technologies, University of Salento, 73100 Lecce, LE, Italy; greta.mastronardi@unisalento.it (G.M.); ileana.blanco@unisalento.it (I.B.)
[3] Department of Civil, Environmental, Land, Building Engineering and Chemistry, Polytechnic University of Bari, 70125 Bari, BA, Italy; audreymarianoemi.martellotta@poliba.it (A.M.N.M.); giacomo.scarasciamugnozza@poliba.it (G.S.M.)
[4] Department of Agriculture, Food, Natural Resources and Engineering (DAFNE), University of Foggia, 25 Napoli St., 71100 Foggia, FG, Italy; sergio.castellano@unifg.it
[5] Department of Engineering, University LUM "Giuseppe Degennaro", 70010 Casamassima, BA, Italy; starace@lum.it
* Correspondence: roberto.puglisi@unibas.it (R.P.); pietro.picuno@unibas.it (P.P.); Tel.: +39-3496709551 (R.P.)

Featured Application

The increasing use of plastic nets for crop protection requires in-depth research on their mechanical properties and durability, since the limited durability of plastic nets may also negatively affect agro-ecosystems. Experimental tests on anti-rain and anti-insect net samples subjected to different cycles of artificial ageing indicated a progressive decline in the mechanical properties.

Abstract

Agricultural nets are increasingly used for crop protection, although their long-term outdoor mechanical durability remains poorly investigated. This study evaluates the tensile behavior of five HDPE nets (anti-rain and anti-insect) subjected to accelerated ageing in an artificial chamber for 2, 4, 8, and 12 weeks (approximately corresponding to 3–18 months of natural exposure). Unidirectional tensile tests were performed in both weft (machine) and warp (transversal) directions to determine Maximum Strength (*Fm*), Tensile Stress at Maximum Strength (*Sm*), and Elongation at Maximum Strength (*A*). The results showed pronounced mechanical anisotropy, with differences in elongation between test directions reaching up to 47%, depending on the net structure and thread arrangement. Accelerated ageing caused a progressive reduction in both tensile strength and ductility, with strength losses in some cases reaching 40–45% after 12 weeks of exposure. Based on the nets analyzed in this study, anti-rain nets tended to exhibit higher initial strength values but faster degradation rates, whereas anti-insect nets showed lower initial strength values (1200–1500 N) and a comparatively more stable response over time. These results suggest that the durability of agricultural nets is strongly influenced by structural configuration and load direction. From an engineering perspective, mechanical durability can be considered a key parameter when selecting crop-protection systems intended for long-term field applications.

Keywords: crop protection; anti-insect nets; anti-rain nets; HDPE agrotextiles; plastic degradation; mechanical properties; tensile tests

Academic Editor: Jinsong Bao

Received: 16 February 2026
Revised: 14 April 2026
Accepted: 24 April 2026
Published: 28 April 2026

1. Introduction

In recent years, the increasing frequency of extreme weather events associated with climate change, including heavy rainfall and changes in pest pressure, has driven the development of more effective crop protection strategies [1,2]. Among these, protective nets are increasingly adopted thanks to their ability to mitigate weather-related damage while regulating solar radiation and microclimate conditions [3–9]. The control of precipitation and excess moisture is particularly relevant for sensitive crops such as cherries, kiwis, pomegranates, and grapes, where humid conditions promote fungal diseases and reduce product quality [10–13]. By selectively regulating air and rainwater passage, agricultural nets could influence crop microclimate and potentially improve fruit quality. However, the reduction in phytosanitary treatments is more consistently reported for anti-rain covers based on plastic films or hybrid systems, which provide a more effective barrier against rainfall and pathogen development [14–16]. In addition, these systems can provide direct protection against pests, although insect nets may alter airflow, potentially leading to increased temperature and suboptimal growing conditions, while still maintaining product quality [17–20]. According to FAO, the adoption of protective nets is increasing worldwide [21,22]. Global production of agricultural nets is estimated to be between 1.5 and 2.5 million tons, corresponding to an estimated economic value of between $11.0 and $12.5 billion. Asia-Pacific (led by China and India) is the main producer and consumer, with a market share of around 40%. Europe follows as the second largest market, with a strong focus on sustainability and recycling of end-of-life nets [23–25].

However, the effectiveness of these systems strongly depends on the mechanical performance of the materials and their ability to withstand environmental stresses over time. Modern agricultural nets are complex systems, where materials engineering meets agronomy. Nets used in agriculture can face various critical issues that can compromise the crop and the investment, such as the sail effect, thermal relaxation, mechanical abrasion, and porosity variation, etc. [26]. Advances in materials engineering and structural design provide new strategies to overcome these limitations. Innovative weaving techniques increase stability, while the use of additives and reinforced polymers, new UV stabilizers, and the integration of nanocomposites allow for the production of thinner monofilaments and superior tensile strength [27]. Structural engineering has introduced dynamic tensioning systems with "*controlled release*" using quick-release plates or spring tensioners [28]. Moreover, the use of Computational Fluid Dynamics (CFD) software, capable of simulating airflow through the mesh, allows structures to be designed with an optimized drag coefficient, reducing stress on the support poles during storms [29]. Despite their widespread use, the long-term mechanical durability of agricultural nets remains insufficiently characterized, particularly under photo-oxidative degradation induced by prolonged solar exposure [30–32]. Although several studies have investigated the influence of net geometric parameters on their mechanical and radiometric properties and air permeability, the available results remain partial or not fully systematized [7,33,34]. From a materials standpoint, most commercial agricultural nets are manufactured in high-density polyethylene (HDPE), which undergoes UV-induced photo-oxidation leading to chain scission and embrittlement, ultimately reducing load-bearing capacity and ductility [30,35]. Another critical aspect is the intrinsic anisotropy of woven structures. Although several studies have investigated the mechanical behavior of agricultural nets and the influence of ageing on polymer-based covers, systematic comparative analyses among different commercial net architectures remain limited. Mechanical tests are essential for evaluating the load-bearing capacity and deformation behavior of agricultural nets subjected to uniaxial stress. These properties are related to the stresses experienced during installation and service conditions—such as pre-tensioning, wind action, etc. In addition,

tensile tests allow for the evaluation of directional anisotropy and mechanical degradation, facilitating the comparison and assessment of the reliability of different agricultural net structures.

Nevertheless, the current literature has several limitations. Most studies focus either on the functional performance of the nets (e.g., radiometric or aerodynamic properties) or on the mechanical behavior of polymer films, while systematic investigations specifically addressing the mechanical response of agricultural nets under controlled ageing conditions remain limited. In particular, the interaction between structural parameters (e.g., mesh geometry and filament arrangement) and time-dependent mechanical degradation is not yet fully understood. In this context, this study aims to experimentally evaluate the mechanical behavior of different commercial agricultural nets subjected to accelerated ageing. Specifically, the study investigated the evolution of tensile properties in both warp and weft directions as a function of exposure time, in order to quantify degradation trends and identify the influence of structural parameters on mechanical durability. The results provide useful insights for improving material selection and supporting the design of more durable crop-protection systems.

2. Materials and Methods

2.1. Structural Characterization

Five agricultural nets were selected for the experimental analysis, including materials specifically designed for rain protection and others intended for different agricultural functions. Three nets were classified as "*Anti-Rain*" nets, characterized by relatively low porosity and designed to partially reduce rainwater passage, while two nets were classified as "*Anti-Insect*" nets. All nets were manufactured in HDPE. The functional distinction between the materials was maintained throughout the study phase through a coding system that assigned each net an acronym that reflected its primary intended use: AR for Anti-Rain nets and AI for Anti-Insect nets (Table 1). This approach allowed for a systematic comparison of the physical and mechanical behavior of the different agrotextiles, highlighting the possible relationships between structural configuration and performance under operating conditions. The analyzed nets are commercially available products widely used in agricultural crop-protection systems. In accordance with good scientific practice and to avoid commercial promotion of specific brands, the manufacturers are not explicitly reported. The materials were therefore anonymized through a coding system (AR and AI), while their structural and physical characteristics are fully described to ensure the reproducibility of the experimental procedures. Although the exact formulation of UV stabilizers and additives is proprietary information not disclosed by manufacturers, the investigated materials belong to the typical class of UV-stabilized HDPE agricultural nets commonly used in crop-protection systems. In Figure 1, some samples of the selected nets for the experimental tests are shown (images, with magnification, not to scale).

Table 1. Agrotextiles selected for experimental analysis.

Net ID	Application	Texture Type	Color	Fiber Type	Polymer
AR-1	Anti-rain	Flat woven	Neutral	Round monofilament warp and rhomboid weft thread	HDPE
AR-2	Anti-rain	Flat woven	Neutral	Round monofilament warp and weft in fibrillated raffia tape	HDPE
AR-3	Anti-rain	Flat woven	Neutral (neutral and red) *	Round monofilament warp and weft in fibrillated raffia tape	HDPE
AI-1	Anti–insects	Flat woven	Neutral	Round monofilament warp and weft	HDPE
AI-2	Anti–insects	Flat woven	Neutral	Round monofilament warp and weft	HDPE

* The net features alternating zones, some entirely neutral in color and others also containing red monofilaments.

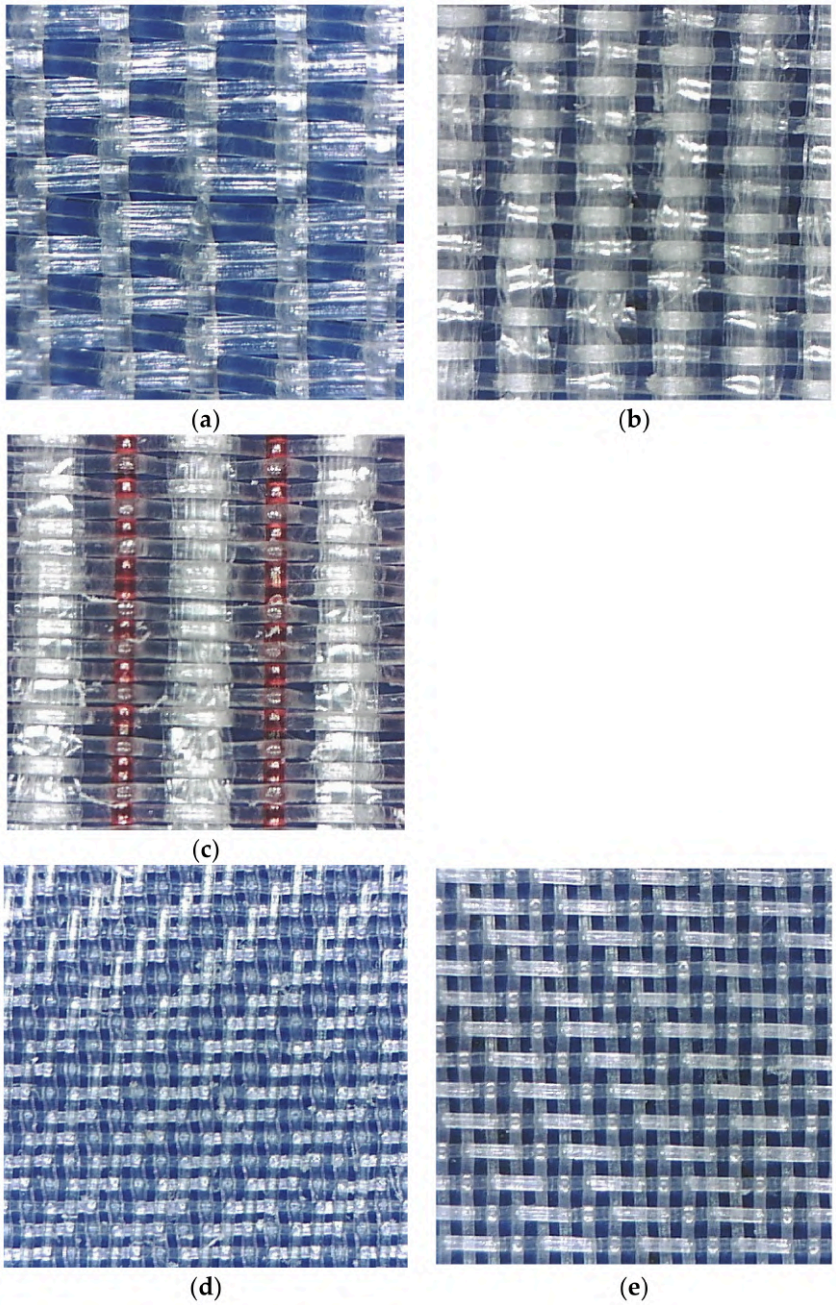

Figure 1. Samples of the nets selected for experimental tests: (**a**) AR–1; (**b**) AR–2; (**c**) AR–3; (**d**) AI–1; (**e**) AI–2. Images are not to scale [6].

The geometric and structural parameters of these nets were determined as reported by Mastronardi et al. 2025 [6], including the number of threads per centimeter in the warp and weft directions, the thread diameters in the warp and weft directions, which may differ depending on the specific net design and manufacturing process, the porosity (ε), and the weight of the net (Table 2).

The thread thickness was measured using a digital micrometer (Mitutoyo, Kanagawa, Japan; model 293–240, Absolute Digimatic), with a resolution of 0.001 mm (range 0–25 mm) and an accuracy of ± 1 µm.

The opening size of the nets was obtained through image-based measurements using a digital microscope (model Dino-Lite AM3013T, Dino-Lite Europe, IDCP B.V., Almere, The Netherlands) and Dino-Capture 2 software, with an accuracy of ± 0.04 mm at $200\times$ magnification (Figure 1).

Table 2. Technical and structural characteristics of the tested agrotextiles.

Net ID	n_{warp} [a] [cm^{-1}]	n_{weft} [b] [cm^{-1}]	d_{warp} [c] [mm]	d_{weft} [d] [mm]	ε [e] [%]	Weight [f] [$g\ m^{-2}$]
AR–1	32.00	7.00	0.280	0.490 **	6.90 *	250
AR–2	20.80	9.44	0.230	0.810 ***	18.00	192
AR–3	30.70	8.30	0.230	0.810 ****	13.20	229
AI–1	31.50	31.00	0.170	0.150	22.30	136
AI–2	31.00	31.00	0.145	0.145	27.00	120

[a] Number of threads in the warp direction, per centimeter; [b] Number of threads in the weft direction, per centimeter; [c] Diameter of the thread in the warp direction; [d] Diameter of the thread in the weft direction; [e] Porosity of the net; [f] Weight of the test sample. * Porosity obtained by analytical calculation; ** Estimated thickness of the weft thread (rhomboidal shaped) measured along the major diagonal; 0.220 mm along the minor diagonal; *** Thickness of the weft thread 0.15 mm; **** Thickness of the weft thread 0.17 mm.

The porosity of the nets (ε, %) was estimated through image analysis. The images were acquired using a 2400 dpi flatbed scanner and processed with Adobe Photoshop (2021, Adobe, San Jose, CA, USA).

The porosity analysis was carried out following a standardized image-processing procedure:

1. image acquisition using a 2400 dpi flatbed scanner;
2. conversion to grayscale;
3. binarization by assigning the net structure to black pixels and voids to white pixels;
4. selection of a representative area (10 cm × 10 cm); and
5. calculation of porosity as the ratio of white pixels to total pixels.

Measurements were performed on at least three representative areas for each net, and the average value was reported [6,36] (Table 2).

For nets characterized by very small open areas, porosity could not be reliably assessed through image analysis. In these cases, porosity was calculated analytically according to Equation (1):

$$\varepsilon = \frac{l_{warp} \times l_{weft}}{(l_{warp} + d_{warp}) \times \left(l_{weft} + d_{weft}\right)} \times 100\ [\%] \quad (1)$$

where d_{warp} and d_{weft} (mm) are the diameters of the monofilaments oriented along the warp and weft directions, respectively, while l_{warp} and l_{weft} (mm) represent the corresponding nets opening lengths between adjacent filaments. This analytical approach was applied only to the AR-1 net, since its high mesh density made image-based porosity estimation negligible or potentially unreliable [6,35].

All measurements were carried out under controlled laboratory conditions (20 ± 1 °C and relative humidity 60 ± 5%) to ensure the repeatability of the experimental procedures.

2.2. Accelerated Ageing Protocol

After selection, the net samples were subjected to an accelerated ageing cycle lasting 2, 4, 8, and 12 weeks, carried out at 20 °C, 60% relative humidity, and 1000 W m^{-2} of irradiance. The tests were performed in an artificial ageing chamber (CO.FO.ME.GRA S.r.l., Milan, Italy, SolarBox model 3000e), installed at the Laboratory of Rural Construction and Agro-Forestry Land Planning—Materials Testing Section—of the University of Basilicata (Italy) (Figure 2). This equipment uses a 2500-Watt xenon lamp to reproduce the solar spectrum (UV–VIS–IR). It achieves twice the irradiance of the sun (up to 1000 W m^{-2}) in the 290–800 nm band, simulating real conditions for accelerated testing [31]. Xenon lamps are considered the most appropriate standard for solar simulation in accelerated ageing tests. The adopted experimental approach is conceptually consistent with the principles described in international weathering standards such as ISO 4892-1, which use

xenon radiation to simulate natural sunlight exposure. However, since these standards are primarily developed for continuous polymeric films and coatings, their direct application to open-structure agrotextiles is not always straightforward. For this reason, the exposure conditions adopted in this study were defined to reproduce realistic outdoor solar radiation conditions typical of Mediterranean agricultural environments. Unlike other light sources, the xenon arc generates a spectrum that covers the entire range of sunlight: UV, visible and infrared (IR). Therefore, while the sun changes intensity throughout the day and seasons, the lamp can maintain a constant intensity, thus significantly accelerating test times. The treatment duration was selected so as to reproduce, in an accelerated form, natural outdoor exposure in Italy, on which an average annual solar irradiance of approximately 4850 MJ m^{-2} (116 kLy) was detected in 2021. Considering that the SolarBox light source operates at a constant irradiance of 1000 W m^{-2}, the cumulative radiant exposure received during the ageing tests can be expressed in MJ m^{-2} by integrating the irradiance over time. Based on this equivalence, the annual solar energy dose corresponds approximately to eight weeks of artificial exposure, as shown by the following calculation:

$$8 \text{ weeks} \times 7 \text{ days week}^{-1} \times 24 \text{ h day}^{-1} \times 3600 \text{ s h}^{-1} \times 1000 \text{ W m}^{-2} = 4838.4 \text{ MJ m}^{-2}$$

Based on this equivalence, cycles of 2, 4, 8, and 12 weeks represent approximately 3, 6, 12, and 18 months of natural exposure to atmospheric agents, respectively. This conversion should be interpreted as an approximate energetic equivalence, rather than a direct field-time correspondence, since the spectral distribution of the radiation emitted by the lamp (especially the UV fraction) is slightly different from natural sunlight. Indeed, while an unfiltered xenon lamp emits too much short UV, which are not representative of terrestrial solar radiation, in this equipment some optical filters are used to remove wavelengths below approximately 290 and 300 nm, making the emitted spectrum comparable, although not identical, to natural sunlight. These experimental conditions were specifically defined for this research, as there is currently no specific ISO/ASTM standard dedicated to the accelerated ageing of nets. Available regulations provide general guidance for plastic materials and degradation tests, but they would require non-trivial adaptations to take into account the specific characteristics of nets and natural outdoor operating conditions, including interaction with rain and agrochemicals [31].

Figure 2. CO.FO.ME.GRA SolarBox 3000e artificial ageing chamber.

2.3. Tensile Tests

The five nets, both unaged and subjected to different accelerated ageing durations, were evaluated by uniaxial tensile tests, performed with a universal testing machine equipped with a 10 kN load cell (Galdabini S.p.A., Cardano al Campo, Italy, Model PMA10). The measurements were conducted at the Laboratory of Rural Construction and Agricultural-Forestry Land Planning of the University of Basilicata (Materials Testing Section), maintaining controlled thermo-hygrometric conditions (20 °C; relative humidity 60 ± 5%) (Figure 3).

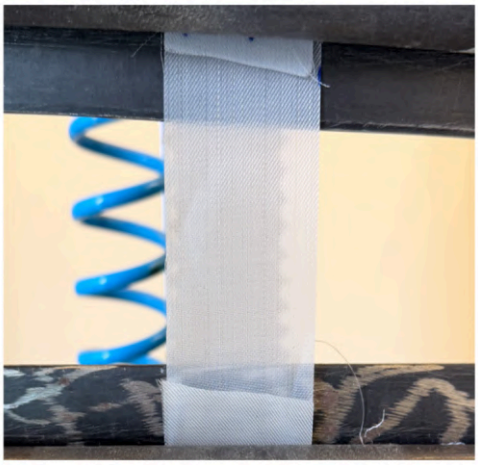

Figure 3. Tensile test with Galdabini PMA10 universal testing machine.

The test specimens were obtained by cutting directly from the net samples, with a width of 50 mm, length of 300 mm, and gauge length of 200 mm, in accordance with UNI 9405/EN ISO 13934-1:2013 [37,38]. During the tensile tests, no breakage occurred at the jaws. The method is particularly suitable for open-structured materials, as it evaluates the entire width of the test piece, reducing the influence of any local irregularities in the net structure. Tensile tests were conducted at a crosshead speed of 200 mm min^{-1}, as required for technical fabrics and materials with non-linear deformation behavior.

For each net, five independent specimens were tested in each direction (weft and warp) (Table 3), resulting in n = 5 replicates per direction for unaged samples, in accordance with UNI 9405/EN ISO 13934-1:2013 [37,38]. The mechanical parameters obtained for the new nets are reported as mean ± standard deviation, calculated from the five replicates tested in each direction. For aged nets, due to the limited capacity of the artificial ageing chamber, only one specimen per direction was tested for each ageing condition. Therefore, the results for aged samples are presented as indicative trends rather than statistically representative values. The analysis focused on the evolution of mechanical behavior over time rather than on inferential statistical comparisons.

Table 3. Test plan for tensile tests on new and artificially aged nets.

Condition	Ageing Time (Weeks)	Test Direction	Number of Specimens (n)
New Nets (AR-1, AR-2, AR-3, AI-1, AI-2)	0	Weft (machine direction)	5
	0	Warp (transversal direction)	5
Aged (AR-1, AR-2, AR-3, AI-1, AI-2)	2, 4, 8, 12	Weft (machine direction)	1
	2, 4, 8, 12	Warp (transversal direction)	1

The results were expressed as Maximum Strength (*Fm*) [N] and Elongation at Maximum Strength (*A*) [%]. In addition to Maximum Strength (*Fm*), the Tensile Stress at

Maximum Strength (*Sm*) [N mm^{-2}] was calculated in order to normalize the load-bearing capacity with respect to the equivalent resistant cross-sectional area of the filaments within the specimen width (50 mm). It is worth noting that the nets analyzed are comparable to non-homogeneous and anisotropic materials. *Sm* was calculated as the ratio between the Maximum Strength *Fm* and the resistant area (A_{res}), according to Equation (2):

$$Sm = \frac{Fm}{A_{res}} \text{ [N mm}^{-2}\text{]} \quad (2)$$

where A_{res} [mm^2] represents the equivalent resistant cross-sectional area of the net, calculated based on the number of load-bearing filaments within the specimen width and their nominal cross-sectional area. For round monofilaments, the filament cross-sectional area was calculated assuming a circular geometry. For AR-1 weft threads, characterized by an approximately rhomboidal rounded section, the cross-sectional area was calculated as elliptical. For AR-2 and AR-3 weft threads, composed of fibrillated raffia tapes, the cross-sectional area was calculated as tape width × tape thickness. Maximum Strength (*Fm*) represents the maximum force recorded when a test specimen is subjected to tensile loading until rupture during a tensile test under the specified conditions [37]. It corresponds to the peak of the load–elongation curve and indicates the load-bearing capacity of the material that the sample is able to withstand during the tensile test, before reaching the point of structural collapse. *Fm* is a key parameter for assessing the mechanical strength of the mesh both during installation (tensioning) and during operation, when it is subjected to loads from wind, rain accumulation, and mechanical stresses induced by the support structure. Elongation at Maximum Strength (*A*) indicates the percentage elongation of the sample at the point where the maximum load *Fm* is reached and measures the deformability of the material before collapse. This parameter describes the material's ability to deform under load. High values of (*A*) indicate more ductile and elastic behavior, while low values indicate a more rigid or brittle material. Descriptive statistics (mean and standard deviation) were calculated for unaged samples. Linear regression analysis was applied to mean values to evaluate degradation trends over time. Statistical analysis was performed using Excel's Analysis ToolPak (Microsoft® Excel® for Microsoft 365 MSO, Version 2509, Redmond, WA, USA). A formal significance threshold was not applied due to the limited number of replicates for aged samples.

2.4. Data Processing and Degradation Indicators

To evaluate the mechanical degradation of the investigated nets during artificial ageing, tensile strength values measured at each ageing stage were expressed as strength retention (SR) relative to the unaged condition. The strength retention (SR) was calculated according to Equation (3):

$$\mathbf{SR_{t_i}} = \frac{\mathbf{Fm_{t_i}}}{\mathbf{Fm_{t_0}}} \times 100 \text{ [\%]} \quad (3)$$

where i is the number of ageing weeks in the range [0, 12], $\mathbf{Fm_{t_i}}$ is the maximum tensile strength [N] after ageing time $\mathbf{t_i}$, and $\mathbf{Fm_{t_0}}$ is the maximum tensile strength [N] of the unaged sample. In addition, the cumulative strength loss (%) at each ageing stage $\mathbf{t_i}$ was calculated as the percentage reduction of tensile strength with respect to the initial value, according to Equation (4):

$$(\mathbf{Strength\ loss})_{\mathbf{t_i}} = \mathbf{100} - \mathbf{SR_{t_i}} \text{ [\%]} \quad (4)$$

3. Results

3.1. Mechanical Behavior of Unaged Nets

Table 4 reports the results of the tensile tests on the five different nets tested in unaged conditions. The tensile response is clearly related to the intrinsic heterogeneity and anisotropy of the tested net structures. In most cases, the warp direction showed notably higher *Fm* values than the weft direction, particularly for AR-1 (3062.90 ± 20.12 N in the warp, vs. 975.00 ± 13.51 N in the weft direction), suggesting a reinforced load-bearing structure along the warp thread system. A similar trend, although less pronounced, was observed for AI-1 and AR-3, where the warp strength exceeded that of the weft, suggesting that thread arrangement and thread density contribute substantially to the overall mechanical performance. On the other hand, AI-2 showed an opposite hierarchy, with a higher *Fm* in the weft (1587.85 ± 9.79 N) than in the warp (1120.02 ± 3.13 N), indicating that the predominance of the warp over the weft is product-specific and depends on the net manufacturing design (thread geometry, density, and load distribution mechanism). AR-2 showed an almost-isotropic strength behavior (1388.22 ± 15.49 N in the weft vs. 1409.02 ± 18.70 N in the warp), indicating a more balanced structural configuration between the two directions. The values of *Sm* provided additional insight into the mechanical response of the nets by accounting for differences in filament cross-sectional area and structural density, allowing a more consistent comparison among nets with different architectures. The resulting *Sm* values, which are generally quite high for a plastic material, can be attributed to stretching and stabilization processes through thermal treatments, both during cooling and heating, which increase the tensile strength of the filaments. The high *Sm* value for the AI-2 net in the weft direction could be attributed to repeated thermal treatments of the filament, even at low stretching speeds. The minimum *Sm* values observed for AR-2 and AR-3 are attributable to the different structure of the weft filament, which consists of fibrillated raffia tape with a rectangular cross-section. The lower *Sm* values compared to other meshes are due to the cutting of the raffia strip during the processing/fibrillation of the raffia (longitudinal cuts), which is an industrial process aimed at producing a material that is easier to work with during weaving and installation phases.

Table 4. Maximum Strength (*Fm*, mean ± SD) [N], Tensile Stress at Maximum Strength (*Sm*, mean ± SD) [N mm^{-2}] and Elongation at Maximum Strength (*A*, mean ± SD) [%] measured by unidirectional tensile tests on unaged nets (n = 5) in weft (machine) and warp (transversal) directions.

Name	N° Sample	Weft *Fm* [N]	Weft *Sm* [N mm^{-2}]	Weft *A* [%]	Warp *Fm* [N]	Warp *Sm* [N mm^{-2}]	Warp *A* [%]
AR-1	5	975.00 ± 13.51	329.19 ± 4.56	18.58 ± 0.49	3062.90 ± 20.12	310.89 ± 2.04	24.77 ± 0.56
AR-2	5	1388.22 ± 15.49	242.07 ± 2.70	16.62 ± 0.79	1409.02 ± 18.70	326.09 ± 4.33	31.60 ± 0.95
AR-3	5	1754.22 ± 35.34	306.97 ± 6.18	18.88 ± 0.41	2409.24 ± 39.73	377.77 ± 6.23	35.46 ± 0.77
AI-1	5	1068.02 ± 2.96	389.92 ± 1.08	26.94 ± 0.59	1545.41 ± 12.93	432.29 ± 3.62	29.42 ± 0.69
AI-2	5	1587.85 ± 9.79	620.37 ± 3.82	24.91 ± 0.52	1120.02 ± 3.13	437.59 ± 1.22	36.52 ± 0.77

3.2. Effect of Accelerated Ageing on Mechanical Properties

Tables 5–9 show the evolution of the mechanical parameters, namely, Maximum Strength, *Fm* [N], *Sm* [N mm^{-2}], and Elongation at Maximum Strength, *A* [%], of the five nets subjected to artificial ageing. Overall, all nets showed a progressive reduction in mechanical performance with increasing ageing time, although with different degradation rates depending on the structure and the material configuration. It can be deduced that the anti-ageing treatments applied to the raw material used in the production of the nets' threads are generally comparable across the various nets analyzed, which were manufactured by different companies. AR-1 (Table 5) exhibited marked mechanical anisotropy, with significantly higher strength in the warp direction than in the weft direction. Artificial age-

ing induced a progressive reduction in maximum strength in both directions, with a more pronounced decrease in the warp direction. Elongation at maximum strength decreased in the weft direction, indicating a loss of ductility, whereas a slight increase is observed in the warp direction, which may suggest a redistribution of stresses within the filament network. Due to the high density of the warp threads (32 cm^{-1}), the warp direction shows the highest initial strength, but also more pronounced degradation (−42% after 12 weeks). While the weft direction showed a progressive loss of ductility, the warp direction showed an increase in elongation at maximum strength, which may be associated with a reduction in stiffness and a redistribution of stresses within the load-bearing threads. Overall, the data suggest that the AR-1 net, while providing high mechanical performance in its initial state, shows relatively rapid degradation under artificial ageing.

Table 5. (*Fm*) Maximum Strength [N], Tensile Stress at Maximum Strength (*Sm*) [N mm^{-2}], and (*A*) Elongation at Maximum Strength [%], in weft/machine direction and warp/transversal direction of AR-1 nets.

Test	Name	Weft *Fm* [N]	Weft *Sm* [N mm^{-2}]	Weft *A* [%]	Warp *Fm* [N]	Warp *Sm* [N mm^{-2}]	Warp *A* [%]
Aged 2 w	AR-1	905.02	305.56	17.41	2721.02	276.19	20.85
Aged 4 w	AR-1	802.45	270.93	17.46	2502.61	254.02	21.57
Aged 8 w	AR-1	688.21	232.36	17.72	2075.35	210.65	23.24
Aged 12 w	AR-1	613.66	207.19	15.91	1773.11	179.97	24.88

Table 6. (*Fm*) Maximum Strength [N], Tensile Stress at Maximum Strength (*Sm*) [N mm^{-2}], and (*A*) Elongation at Maximum Strength [%], in weft/machine direction and warp/transversal direction of AR-2 nets.

Test	Name	Weft *Fm* [N]	Weft *Sm* [N mm^{-2}]	Weft *A* [%]	Warp *Fm* [N]	Warp *Sm* [N mm^{-2}]	Warp *A* [%]
Aged 2 w	AR-2	1251.31	218.20	16.32	1270.61	294.06	30.66
Aged 4 w	AR-2	1058.30	184.54	14.61	1094.01	253.19	28.75
Aged 8 w	AR-2	894.21	155.93	14.38	915.65	211.91	26.91
Aged 12 w	AR-2	739.25	128.91	12.41	790.97	183.05	24.41

Table 7. (*Fm*) Maximum Strength [N], Tensile Stress at Maximum Strength (*Sm*) [N mm^{-2}], and (*A*) Elongation at Maximum Strength [%], in weft/machine direction and warp/transversal direction of AR-3 nets.

Test	Name	Weft *Fm* [N]	Weft *Sm* [N mm^{-2}]	Weft *A* [%]	Warp *Fm* [N]	Warp *Sm* [N mm^{-2}]	Warp *A* [%]
Aged 2 w	AR-3	1503.51	263.10	15.71	2053.52	321.99	31.25
Aged 4 w	AR-3	1347.72	235.84	14.63	1859.61	291.59	32.18
Aged 8 w	AR-3	1086.84	190.19	13.91	1452.02	227.68	27.91
Aged 12 w	AR-3	917.01	160.47	13.26	1210.41	189.79	27.56

Table 8. (*Fm*) Maximum Strength [N], Tensile Stress at Maximum Strength (*Sm*) [N mm^{-2}], and (*A*) Elongation at Maximum Strength [%], in weft/machine direction and warp/transversal direction of AI-1 nets.

Test	Name	Weft *Fm* [N]	Weft *Sm* [N mm^{-2}]	Weft *A* [%]	Warp *Fm* [N]	Warp *Sm* [N mm^{-2}]	Warp *A* [%]
Aged 2 w	AI-1	882.82	322.31	24.46	1344.45	376.08	26.13
Aged 4 w	AI-1	818.91	298.97	24.37	1204.73	336.99	25.06
Aged 8 w	AI-1	703.44	256.82	22.93	1035.37	289.62	24.43
Aged 12 w	AI-1	617.32	225.38	21.91	862.12	241.16	22.87

Table 9. (*Fm*) Maximum Strength [N], Tensile Stress at Maximum Strength (*Sm*) [N mm^{-2}], and (*A*) Elongation at Maximum Strength [%], in weft/machine direction and warp/transversal direction of AI-2 nets.

Test	Name	Weft *Fm* [N]	Weft *Sm* [N mm^{-2}]	Weft *A* [%]	Warp *Fm* [N]	Warp *Sm* [N mm^{-2}]	Warp *A* [%]
Aged 2 w	AI-2	1410.61	551.12	19.06	1007.62	393.68	31.26
Aged 4 w	AI-2	1373.73	536.72	19.93	934.85	365.25	33.81
Aged 8 w	AI-2	1221.25	477.14	18.26	809.81	316.39	29.61
Aged 12 w	AI-2	1225.51	478.81	17.91	738.15	288.39	28.36

Note: for aged nets, one specimen per direction was tested for each ageing stage.

AR-2 (Table 6) exhibited a more balanced mechanical behavior between the warp and weft directions compared with AR-1. Artificial ageing produces a gradual and monotonic reduction in maximum strength in both directions. Elongation at maximum strength also decreases progressively, indicating a general loss of ductility and structural integrity over time. Overall, the AR-2 net showed intermediate behavior between AR-1 and insect nets, with marked but more regular mechanical degradation over time. This response suggests that, while guaranteeing good initial performance, AR-2 may require careful evaluation of mechanical durability in applications characterized by prolonged exposure to severe environmental conditions.

AR-3 (Table 7) showed high initial mechanical strength, particularly in the warp direction. Artificial ageing causes a progressive reduction in maximum strength in both directions, indicating marked sensitivity to degradation processes. Elongation at maximum strength also decreases with ageing, confirming a progressive loss of ductility associated with the reduction in load-bearing capacity of the threads. Overall, the AR-3 net combined high initial mechanical performance with rapid degradation over time, suggesting a higher sensitivity to ageing compared to AR-1 and AR-2.

AI-1 (Table 8) showed a progressive decline in mechanical performance with increasing ageing time. Both maximum strength and elongation at maximum strength decreased in the weft and warp directions, suggesting gradual embrittlement of the material. Despite the degradation, the warp direction consistently maintained higher strength and deformation capacity than the weft direction.

AI-2 (Table 9) showed a more stable mechanical behavior compared to AI-1. Maximum strength decreased progressively with ageing in both directions, although the weft direction initially exhibited higher resistance than the warp direction. Elongation at maximum strength showed a less regular trend, particularly in the weft direction, which may reflect complex structural responses of the net during degradation.

3.3. Load–Elongation Behavior During Ageing

Figures 4–8 show the load–elongation curves obtained from tensile tests on AR-1, AR-2, AR-3, AI-1, and AI-2 nets, in the weft/machine and warp/transversal directions, for different time durations of artificial ageing. These curves provide a complete representation of the evolution of the mechanical behavior of the nets, allowing simultaneous analysis of initial stiffness, load-bearing capacity, deformability, and failure mode. In all the analyzed configurations, artificial ageing causes a progressive reduction in the maximum sustainable force, accompanied by an earlier onset of failure, as evidenced by the shift of the curves towards lower load and elongation values. This effect is particularly marked at 8 and 12 weeks, suggesting an advanced state of degradation of the polymeric material. The reduction in the area under the curves also suggests a decrease in the energy absorbed up to failure, indicating a progressively more brittle behavior of the material as ageing time increased. AR-1 nets showed not only higher initial curves, particularly in the warp

direction, but also a more rapid loss of performance with ageing, as evidenced by the marked reduction in maximum strength and the shortening of the post-elastic phase. In contrast, AR-2 nets showed closer curves among the different ageing stages, suggesting a more regular and gradual mechanical degradation. This behavior is consistent with a more balanced net structure, as already highlighted by the tabular results, and indicates greater stability of mechanical behavior over time.

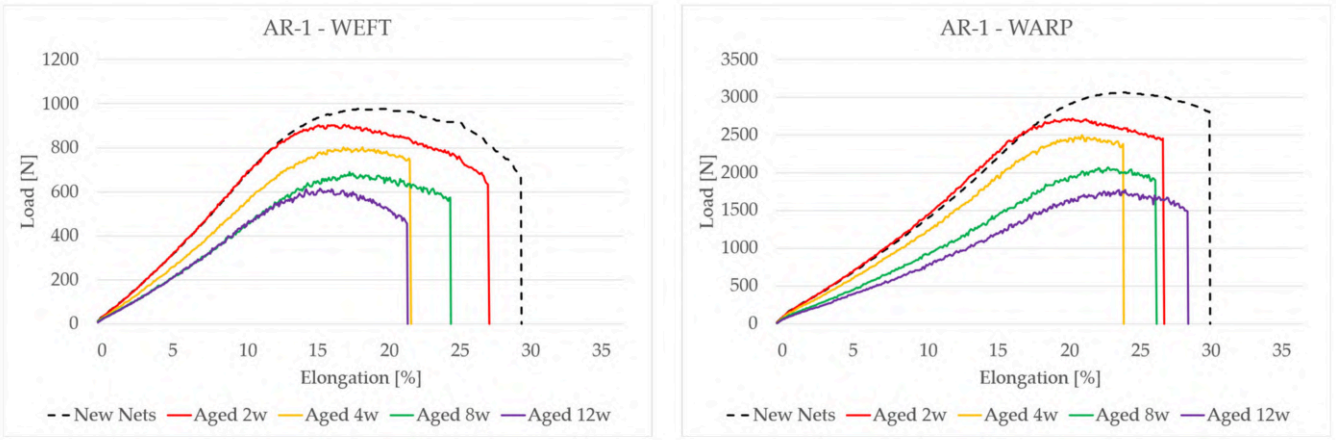

Figure 4. Load–elongation curves of AR-1 net in weft direction (**a**) and warp direction (**b**) at different artificial ageing times.

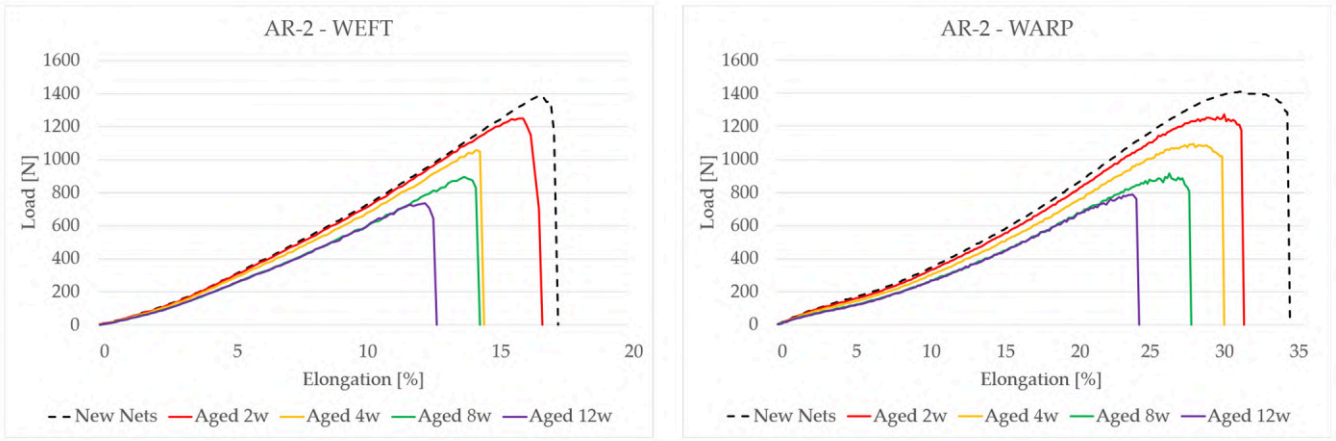

Figure 5. Load–elongation curves of AR-2 net in weft direction (**a**) and warp direction (**b**) at different artificial ageing times.

The comparison between the two different test directions highlights clear mechanical anisotropy. In the warp direction, the curves show higher initial slopes, indicating greater stiffness and higher maximum strength, consistent with the primary structural role of the longitudinal threads. However, ageing causes a more pronounced reduction in maximum strength in the warp direction, especially for AR-1 nets, which may suggest that the load-bearing threads are more susceptible to photo-oxidation and structural degradation. In the weft direction, the curves are generally lower and characterized by lower load-bearing capacity, although in some cases they show a more gradual reduction in elongation, indicating a more progressive response to degradation.

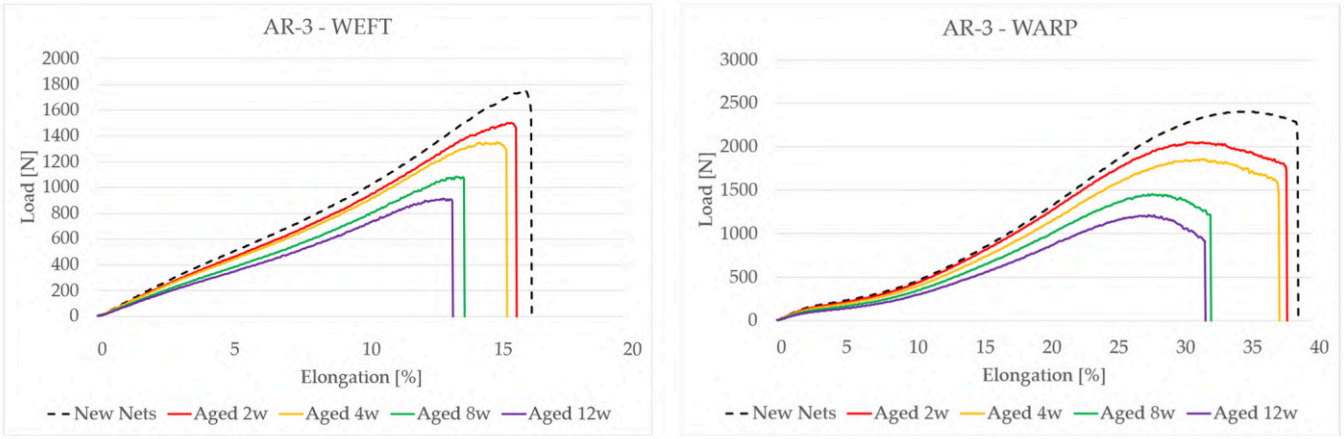

(**a**) (**b**)

Figure 6. Load–elongation curves of AR-3 net in weft direction (**a**) and warp direction (**b**) at different artificial ageing times.

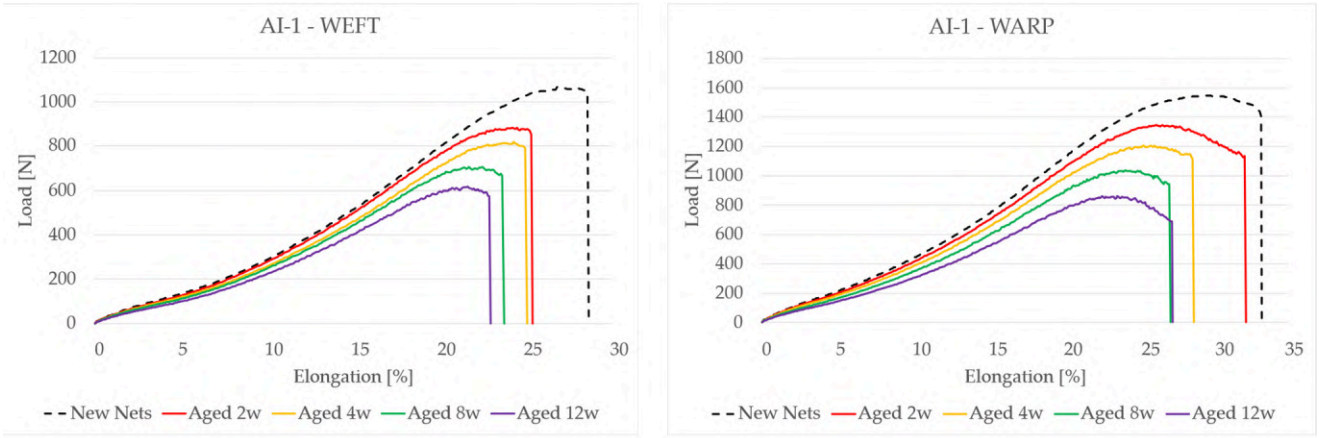

(**a**) (**b**)

Figure 7. Load–elongation curves of AI-1 net in weft direction (**a**) and warp direction (**b**) at different artificial ageing times.

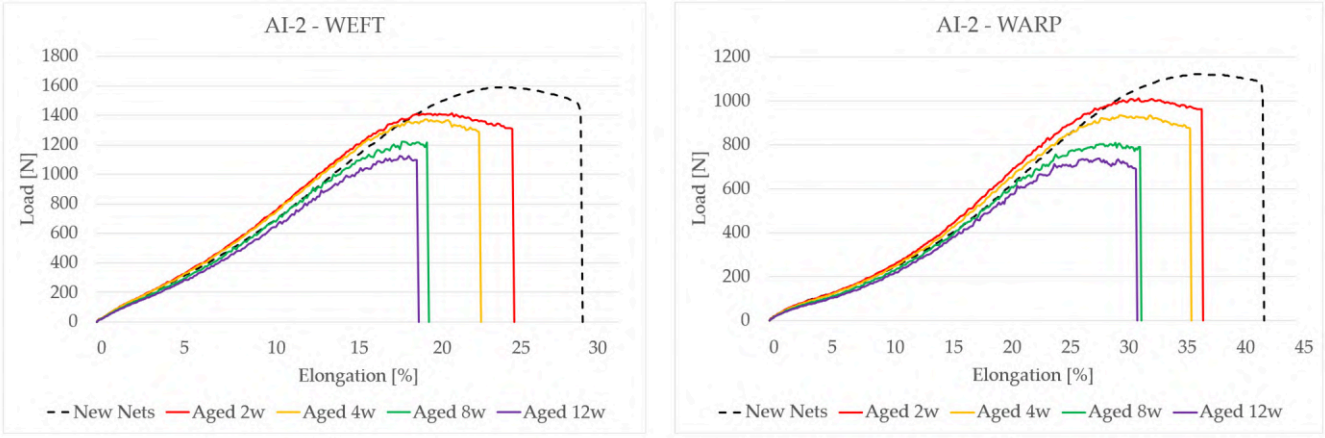

(**a**) (**b**)

Figure 8. Load–elongation curves of AI-2 net in weft direction (**a**) and warp direction (**b**) at different artificial ageing times.

Figure 9 compares the Maximum Strength (*Fm*) of the different nets in the weft and warp directions under unaged conditions and after 12 weeks of ageing, corresponding

to approximately 18 months of natural outdoor exposure. In all cases, a reduction in strength was observed after accelerated exposure, with particularly marked decreases for AR-1, AR-3, and AI-1. The AR-1 net in the warp direction showed the highest values both in the unaged condition and after ageing, compared with all other tested nets, whereas AR-2 showed a more moderate decrease and a more balanced behavior between the two directions.

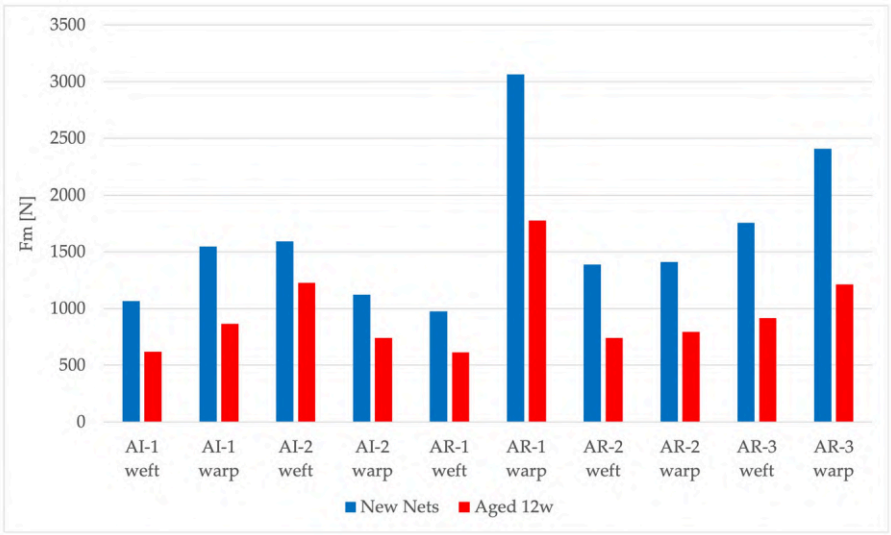

Figure 9. Comparison of Maximum Strength (*Fm*) measured in unidirectional tensile tests for the analyzed nets in the weft (machine) and warp (transversal) directions, under unaged conditions and after 12 weeks of accelerated ageing.

3.4. Strength Retention and Cumulative Strength Loss During Artificial Ageing

To facilitate a comparison of the investigated nets, the evolution of maximum tensile strength during artificial ageing was also expressed in terms of strength retention (%), calculated relative to the unaged condition. Figures 10 and 11 show the strength retention trends of the investigated nets as a function of ageing time. A progressive reduction in tensile strength was observed for all the nets, confirming the mechanical degradation induced by prolonged UV exposure. To highlight the general degradation behavior, the average strength retention values were calculated separately for the warp and weft directions. Linear regression analysis was applied to the mean strength retention values calculated separately for the weft and warp directions as a function of ageing time. The resulting coefficients of determination (R^2 ranging from 0.89 to 0.97) indicate that, within the investigated ageing interval, the reduction in tensile strength follows an approximately linear decay trend. Individual markers in Figures 10 and 11 represent the experimental values measured for each net type, while the dotted lines correspond to the linear regression calculated from the directional mean values. The red dotted line refers to the linear regression of the mean values in the weft direction, whereas the blue one refers to the linear regression of the mean values in the warp direction. Overall, the results suggest that the mechanical degradation of agricultural nets under accelerated ageing follows a time-dependent decrease in tensile strength, with similar degradation trends observed for AR nets in both warp and weft directions (regression slopes ranging from −3.61 to −3.71 percentage points per week). In contrast, AI nets exhibited a slightly lower degradation rate compared to AR nets (regression slopes ranging from −2.52 to −3.14 percentage points per week).

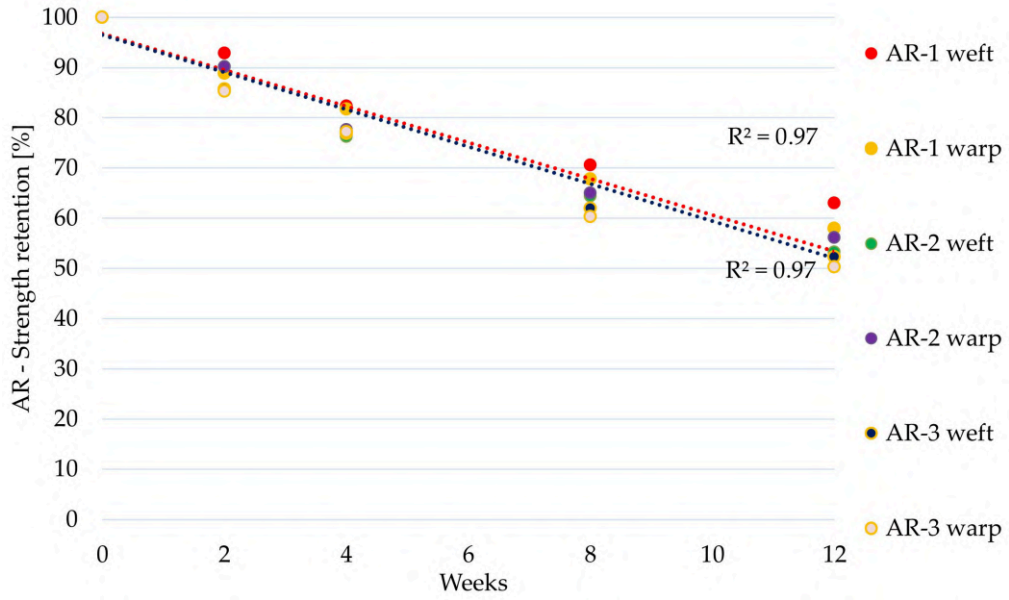

Figure 10. Strength retention (%) of anti-rain nets (AR-1, AR-2 and AR-3) during artificial ageing in the warp and weft directions.

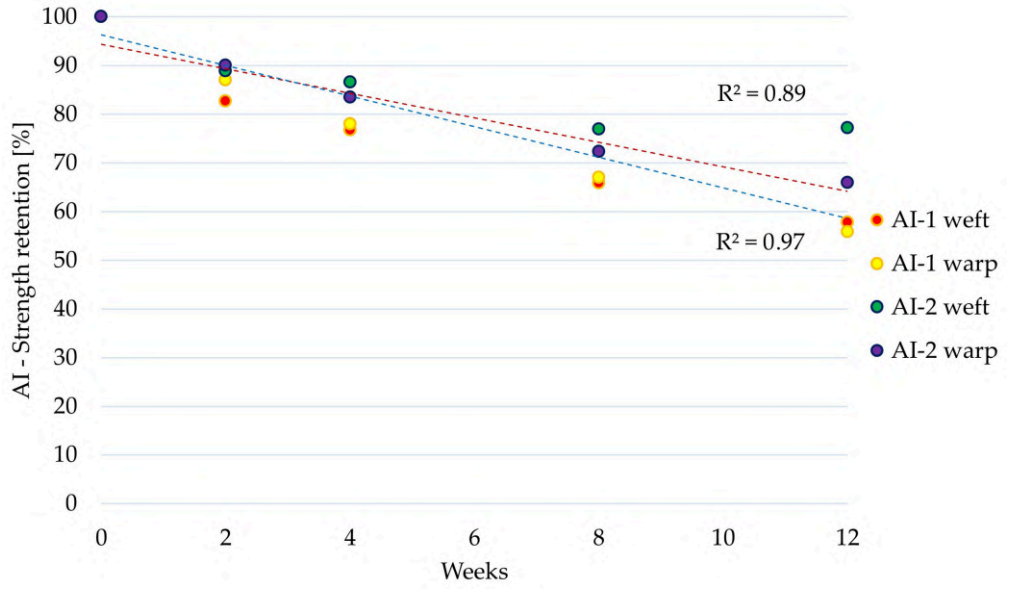

Figure 11. Strength retention (%) of anti-insect nets (AI-1 and AI-2) during artificial ageing in the warp and weft directions.

To provide a clearer representation of the degradation process, the evolution of tensile strength was also expressed as cumulative strength loss (%) relative to the unaged condition. This parameter represents the progressive reduction in mechanical performance during artificial ageing and allows a direct comparison among the investigated nets. Figure 12 shows the cumulative strength loss of the analyzed nets as a function of ageing time. A progressive increase in strength loss was observed for all the nets, indicating a continuous degradation of the polymeric structure during exposure. The mean values calculated for the warp and weft directions show a nearly linear increase in strength loss over time, as confirmed by the high coefficients of determination obtained from linear regression analysis (R^2 = 0.98–0.99). These regressions should be interpreted as descriptive trend indicators rather than predictive degradation models, due to the limited number of ageing levels and the absence of replicate specimens for aged conditions.

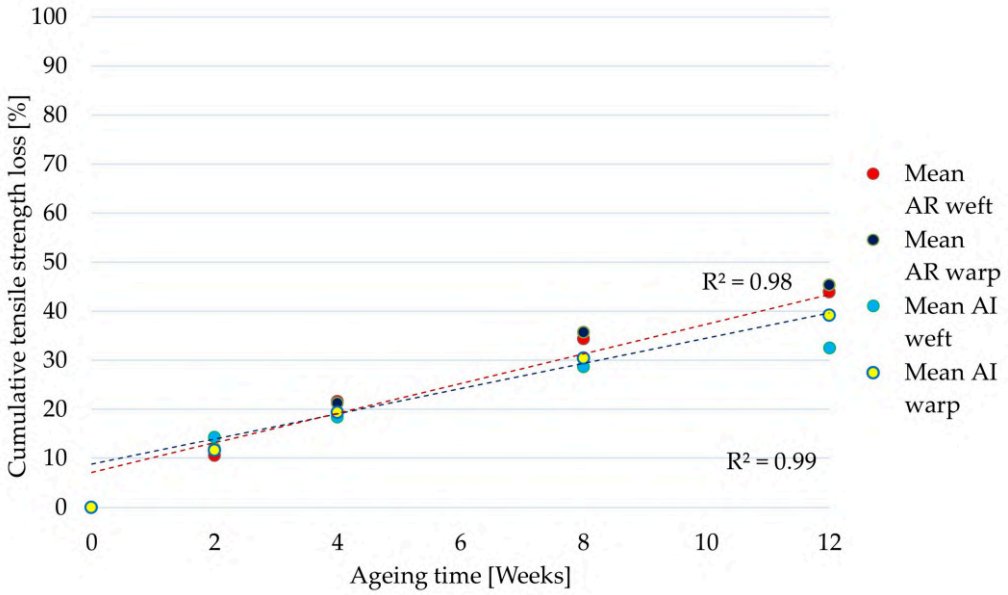

Figure 12. Cumulative tensile strength loss (%) of the investigated agricultural nets during artificial ageing. Markers represent mean values for the weft and warp directions of anti-rain (AR) and anti-insect (AI) nets, while dotted lines indicate linear regression trends.

3.5. Relationship Between Geometrical Porosity (ε) and Mean Maximum Strength (Fm_{mean}) of the Investigated Nets

Geometrical porosity (ε) represents an important structural parameter of nets, describing the ratio between the open area of the mesh and the total surface of the net. Porosity is typically associated with functional properties of agricultural nets, such as air permeability, light transmission, and rainwater passage. However, the geometrical configuration of the textile structure may also influence the mechanical behavior of the material. To explore this aspect, the relationship between geometrical porosity and the mean tensile strength (Fm_{mean}) of the investigated nets was analyzed. The mean tensile strength (Fm_{mean}) was calculated as the average of the maximum tensile strength values measured in the warp and weft directions. Figure 13 shows the correlation between porosity and the corresponding mean tensile strength values obtained through linear regression analysis. The results suggest that the mechanical behavior of agricultural nets is influenced by the combined effect of porosity and the structural characteristics of the textile architecture. In general, nets with larger open areas may exhibit lower tensile strength because the load is distributed over a smaller number of load-bearing filaments. However, this relationship is not strictly proportional. In some cases, such as insect-proof nets, high porosity can coexist with a high number of filaments per unit length combined with a reduced filament diameter. In these configurations, load transfer within the textile structure depends not only on the open area, but also on the thread density, filament diameter, and mesh architecture. Therefore, the mechanical strength of agricultural nets results from the interaction between multiple structural parameters rather than porosity alone.

A moderate relationship between the two parameters was observed ($R^2 = 0.74$), indicating that porosity alone does not fully explain the variability in mechanical strength. Nevertheless, this relationship should be interpreted with caution, as the mechanical behavior of agrotextiles is influenced by multiple structural and material parameters, including filament diameter, thread arrangement, weaving pattern, and polymer characteristics. Consequently, porosity can be considered one of the structural factors potentially affecting the mechanical response of agricultural nets, although it does not represent the sole parameter governing their tensile performance.

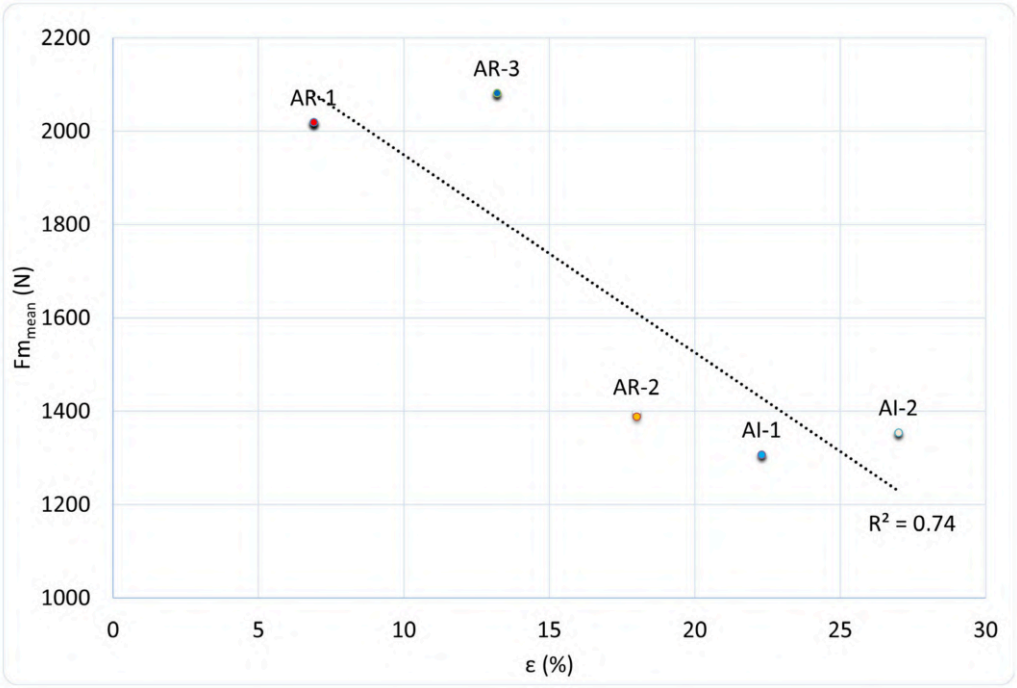

Figure 13. Relationship between geometrical porosity (ε) and mean tensile strength (Fm_{mean}) of the investigated nets.

4. Discussion

The mechanical behavior and durability of different agricultural nets subjected to accelerated artificial ageing were analyzed to investigate the relationships between net type, structural configuration, load direction, and degradation trends. The results provide an overall assessment of how rain nets (AR) and insect nets (AI) respond to prolonged exposure to simulated environmental conditions, representative of agricultural contexts in southern Italy. Our findings are in line with previous studies, which showed that agricultural nets exhibit strong directional anisotropy and that ageing can significantly reduce tensile performance depending not only on polymer type (HDPE) but also on thread geometry and weave architecture, suggesting that mechanical durability depends strongly on net-specific structural characteristics [1,39].

The mechanical trends observed in this study are consistent with previous evidence showing that agricultural nets behave as orthotropic structures, with a strong dependence of the tensile response on the test direction and mesh architecture. Picuno et al. [40] reported that the mechanical performance of HDPE nets is influenced by the number, diameter, and arrangement of threads in the warp and weft directions, and that the ratio between maximum strength and elongation at maximum strength can vary considerably depending on weaving technology and thread density.

A key finding from the current dataset is the different sensitivity of the nets to ageing, despite belonging to the same polymer family. While AR-1 and AR-3 showed substantial losses in maximum strength after 12 weeks (reducing their initial strength by about half in several configurations), AR-2 exhibited a more gradual decay and a more balanced response between directions. This behavior suggests that mechanical durability is influenced not only by polymer type, but also by the stabilizer formulation, thread geometry (monofilament vs. tape), weave compactness, and stress distribution within the net structure. Similar trends were reported by Giannoulis et al., [7], where improvements in functional properties such as ventilation or radiometric performance were associated with reductions in mechanical durability, highlighting a trade-off between functional efficiency and structural resistance.

A slight increase in elongation at maximum strength was observed in some cases during the early stages of ageing (e.g., AR-1, AR-3 and AI-2). This behavior may be associated with structural rearrangements within the net, including geometric reconfiguration of the mesh and possible relaxation effects in the polymer filaments. However, no direct physico-chemical analyses were performed in this study, and therefore these mechanisms should be regarded as possible interpretations rather than confirmed processes [31].

For several analyzed nets, although not in all cases, the artificial ageing resulted in a progressive reduction in Maximum Strength (*Fm*) and Elongation at Maximum Strength (*A*), both in the weft and warp directions. This behavior is consistent with the known effects of photo-oxidative degradation of polyethylene-based polymeric materials, which involve macromolecular chain scission, a reduction in molecular weight, and progressive embrittlement. A comparison between anti-insect (AI) and anti-rain (AR) nets highlighted substantial differences in mechanical behavior. The *Sm* values suggest that the differences in the absolute strength values (*Fm*) among the warp and weft directions and between different nets are largely governed by structural parameters such as filament diameter and thread density, rather than by intrinsic material strength alone.

Insect nets exhibited lower initial strength values but a more stable response over time, with less pronounced degradation trends. In contrast, rain nets showed not only higher initial mechanical performance, particularly in the warp direction, but also greater sensitivity to degradation processes, with strength losses reaching approximately 45–50% after 12 weeks.

This behavior can be reasonably attributed to the structural characteristics of rain nets, including higher thread density and lower porosity, which could promote stress concentration phenomena and potentially enhance the effects of UV-induced degradation. The comparison between test directions confirmed the presence of marked mechanical anisotropy. The warp direction generally exhibited higher maximum strength and stiffness, consistent with the primary load-bearing role of the longitudinal threads. However, this trend was not observed in AI-2, where the weft direction showed higher strength values, reflecting a more balanced structural configuration.

Load–elongation curves further indicated that ageing affects not only the ultimate strength but also failure mechanisms. In particular, the reduction in the area under the curves suggests a decrease in the energy observed at failure, indicating a transition toward more brittle behavior. From an engineering perspective, this progressive embrittlement may influence the service life of agricultural nets under field conditions. Reduced ductility may increase the likelihood of local filament rupture under dynamic loads such as wind, rainfall, and mechanical stresses from the supporting structures.

When analyzing load–elongation curves, it should be noted that agricultural nets do not exhibit a well-defined linear elastic region comparable to that of homogeneous polymer films. The initial portion of the curve is strongly influenced by the geometric reorganization of the mesh, including the rotation and alignment of the threads under tensile loading. Although elastic modulus values have been reported for several agricultural nets in the literature [4,7], their determination may strongly depend on the strain interval considered and on the structural reconfiguration of the mesh during the initial loading stage. Therefore, the mechanical response of nets results from the combined effect of filament elasticity and structural deformation of the mesh, leading to progressive load transfer among threads until failure.

A comparison between agricultural nets and plastic films can further clarify the observed mechanical behavior. Although both materials are typically polyethylene-based, their structural configuration leads to fundamentally different responses under tensile loading. Plastic films behave as continuous materials, where stress distribution is uniform

and failure is typically characterized by rapid crack propagation once a defect is present. In contrast, agricultural nets are discontinuous structures composed of interconnected filaments, where the load is distributed among multiple threads. This structural configuration allows for progressive failure mechanisms and local damage without immediate global collapse. Furthermore, the mechanical response of nets is strongly influenced by geometric deformation of the mesh prior to filament stretching, resulting in an apparently higher deformability compared to films. These differences highlight the importance of considering structural architecture when evaluating the mechanical durability of agrotextiles.

Some limitations of this study should be acknowledged. First, due to the limited capacity of the ageing chamber, only one specimen per direction was tested for aged conditions, which limits the possibility of performing a statistical evaluation of variability at each ageing stage. Second, although the accelerated ageing protocol provides an energetic equivalence to natural exposure, it does not fully reproduce real environmental conditions, such as fluctuating temperature, humidity, and combined mechanical stresses. Finally, no physico-chemical analyses (e.g., FTIR, DSC or SEM) were performed to directly investigate polymer degradation mechanisms. Therefore, the interpretation of degradation processes is based on mechanical evidence and should be considered as indicative rather than definitive. Future studies integrating mechanical, chemical, and microstructural analyses are recommended to provide a more comprehensive understanding of degradation mechanisms.

5. Conclusions

This study investigated the mechanical behavior and durability of different agricultural nets subjected to accelerated ageing, focusing on the influence of structural configuration and load direction on tensile performance. The results indicate that mechanical degradation occurs progressively over time and is strongly dependent on the specific net architecture, including thread arrangement and mesh structure. The findings suggest that mechanical durability represents an important parameter to be considered alongside functional performance, such as protection against rain and insects, in the selection and design of crop-protection systems. In this context, the combined analysis of tensile properties and degradation indicators provides valuable insights into the long-term behavior of agrotextiles. Future research should focus on the investigation of combined ageing factors (e.g., UV radiation, agrochemical exposure, and cyclic mechanical loading), as well as the integration of mechanical, chemical, and microstructural analyses. Moreover, comparisons between accelerated ageing and real field conditions would contribute to improving the reliability of durability assessments and supporting the development of more efficient and resilient agricultural nets.

Author Contributions: Conceptualization, G.S.M., S.C., P.P., G.S. and I.B.; methodology, P.P.; software, R.P.; validation, G.S.M., S.C., P.P., G.M., G.S., R.P. and I.B.; formal analysis, P.P. and R.P.; investigation, R.P.; resources, P.P.; data curation, P.P. and R.P.; writing—original draft preparation, R.P.; writing—review and editing, A.M.N.M., G.S.M., S.C., P.P., G.M., R.P. and I.B.; visualization, P.P. and R.P.; supervision, G.S.M.; project administration, G.S.M. and I.B.; funding acquisition, G.S.M., S.C., P.P. and I.B. All authors have read and agreed to the published version of the manuscript.

Funding: This research was funded by the European Union—Next-GenerationEU—National Recovery and Resilience Plan (NRRP)—MISSION 4 COMPONENT 2, INVESTMENT N. 1.1, CALL PRIN 2022 PNRR D.D. 1409 14-09-2022—Project Title "RESCUE-NETS—RESilience to Climate change in agricultural production under multi-pUrposE NETS"—Cod. Prog. P2022YSF3K—CUP D53D23022120001.

Institutional Review Board Statement: Not applicable.

Informed Consent Statement: Not applicable.

Data Availability Statement: The original contributions presented in this study are included in the article.

Acknowledgments: The authors would like to thank Cosimo Marano, a technical staff member of the DAFE Department at the University of Basilicata, for his assistance in conducting the laboratory tests and mechanical strength tests.

Conflicts of Interest: The authors declare no conflicts of interest. The funders had no role in the design of the study; in the collection, analyses, or interpretation of data; in the writing of the manuscript; or in the decision to publish the results.

References

1. Puglisi, R.; Starace, G.; Lippolis, M.; Picuno, P. Analysis of Spectroradiometric and Mechanical Characteristics of a New Generation of Anti-Rain Agrotextiles. In *Proceedings of the Biosystems Engineering Promoting Resilience to Climate Change—AIIA 2024—Mid-Term Conference*; Sartori, L., Tarolli, P., Guerrini, L., Zuecco, G., Pezzuolo, A., Eds.; Springer Nature: Cham, Switzerland, 2025; pp. 1024–1031.
2. Cogato, A.; Meggio, F.; Migliorati, M.D.A.; Marinello, F. Extreme Weather Events in Agriculture: A Systematic Review. *Sustainability* **2019**, *11*, 2547. [CrossRef]
3. Briassoulis, D.; Mistriotis, A.; Eleftherakis, D. Mechanical Behaviour and Properties of Agricultural Nets—Part I: Testing Methods for Agricultural Nets. *Polym. Test.* **2007**, *26*, 822–832. [CrossRef]
4. Briassoulis, D.; Mistriotis, A.; Eleftherakis, D. Mechanical Behaviour and Properties of Agricultural Nets. Part II: Analysis of the Performance of the Main Categories of Agricultural Nets. *Polym. Test.* **2007**, *26*, 970–984. [CrossRef]
5. Martellotta, A.M.N.; Castellano, S.; Blanco, I.; Mastronardi, G.; Picuno, P.; Puglisi, R.; Scarascia Mugnozza, G. Standard Procedures Proposal of Laboratory Experimental Tests Assessment for Water Permeability of Anti-Rain Agricultural Nets. *Horticulturae* **2025**, *11*, 1253. [CrossRef]
6. Mastronardi, G.; Puglisi, R.; Castellano, S.; Picuno, P.; Martellotta, A.M.N.; Scarascia Mugnozza, G.; Blanco, I. Experimental Evaluation of Anti-Rain Agricultural Nets: Structural Parameters and Functional Efficiency. *Agriculture* **2025**, *15*, 2194. [CrossRef]
7. Giannoulis, A.; Briassoulis, D.; Papardaki, N.-G.; Mistriotis, A. Evaluation of Insect-Proof Agricultural Nets with Enhanced Functionality. *Biosyst. Eng.* **2021**, *208*, 98–112. [CrossRef]
8. Harmanto; Tantau, H.J.; Salokhe, V.M. Microclimate and Air Exchange Rates in Greenhouses Covered with Different Nets in the Humid Tropics. *Biosyst. Eng.* **2006**, *94*, 239–253. [CrossRef]
9. Assogba-Komlan, F.; Ahouangninou, C.; Adegbola, P.; Simon, S.; Ngouajio, M.; Martin, T. Evaluation of the Effect of the Use of Anti-Insect Nets on Vegetable Production in Southern Benin. *Afr. J. Agric. Res.* **2021**, *17*, 1463–1471. [CrossRef]
10. Blanke, M.; Balmer, M. Cultivation of Sweet Cherry under Rain Covers. *Acta Hortic.* **2008**, *795*, 479–484. [CrossRef]
11. Jahani, M.; Zohan, M.S.; Moradinezhad, F.; Khayyat, M.; Mirzaee, M.R. Effects of Shading Nets on Yield, Quality, and Aril Paleness in Pomegranate Cultivars. *Appl. Fruit Sci.* **2025**, *67*, 244. [CrossRef]
12. Moura, L.; Pinto, R.; Rodrigues, R.; Brito, L.M.; Rego, R.; Valín, M.I.; Mariz-Ponte, N.; Santos, C.; Mourão, I.M. Effect of Photo-Selective Nets on Yield, Fruit Quality and Psa Disease Progression in a 'Hayward' Kiwifruit Orchard. *Horticulturae* **2022**, *8*, 1062. [CrossRef]
13. Husni, I.R.; Sudirman, S. The Effect of Using UV Plastic Shade and Soil Amendments in Suppressing the Presence of Thrips Pests on Tomato Plants in Dry Land. *Int. J. Sci. Technol. Manag.* **2025**, *6*, 422–429. [CrossRef]
14. Mupambi, G.; Anthony, B.M.; Layne, D.R.; Musacchi, S.; Serra, S.; Schmidt, T.; Kalcsits, L.A. The Influence of Protective Netting on Tree Physiology and Fruit Quality of Apple: A Review. *Sci. Hortic.* **2018**, *236*, 60–72. [CrossRef]
15. Salvadores, Y.; Bastías, R.M.; Salvadores, Y.; Bastías, R.M. Environmental Factors and Physiological Responses of Sweet Cherry Production under Protective Cover Systems: A Review. *Chil. J. Agric. Res.* **2023**, *83*, 484–498. [CrossRef]
16. Abdel-Ghany, A.M.; Al-Helal, I.M.; Picuno, P.; Shady, M.R. Modified Plastic Net-Houses as Alternative Agricultural Structures for Saving Energy and Water in Hot and Sunny Regions. *Renew. Energy* **2016**, *93*, 332–339. [CrossRef]
17. Formisano, L.; El-Nakhel, C.; Corrado, G.; De Pascale, S.; Rouphael, Y. Biochemical, Physiological, and Productive Response of Greenhouse Vegetables to Suboptimal Growth Environment Induced by Insect Nets. *Biology* **2020**, *9*, 432. [CrossRef]
18. Yu, H.; Tian, S.; Huang, Q.; Chen, J.; Wu, Y.; Wang, R.; Lu, L. An Insect- and Rain-Proof Net Raises the Production and Quality of Chinese Bayberry by Preventing Damage from Insects and Altering Bacterial Communities. *Front. Plant Sci.* **2021**, *12*, 732012. [CrossRef] [PubMed]
19. Vuković, M.; Jurić, S.; Vinceković, M.; Levaj, B.; Fruk, G.; Jemrić, T. Effect of Yellow and Stop Drosophila Normal Anti-Insect Photoselective Nets on Vegetative, Generative and Bioactive Traits of Peach (Cv. Suncrest). *Tarim Bilim. Derg.* **2023**, *29*, 111–121. [CrossRef]

20. Correia, S.; Schouten, R.; Silva, A.P.; Gonçalves, B. Sweet Cherry Fruit Cracking Mechanisms and Prevention Strategies: A Review. *Sci. Hortic.* **2018**, *240*, 369–377. [CrossRef]
21. Nuñez-Rubio, M.; Edo, C.; Gálvez-Blanca, V.; Valenzuela-Lázaro, J.M.; Pulido-Reyes, G.; González-Pleiter, M.; Fernández-García-del-Rincón, L.; Leganés, F.; Fernández-Piñas, F.; Rosal, R. Beyond the Greenhouse: The Spread of Plastic Pollution from an Intensively Cultivated Agricultural Area. *Emerg. Contam.* **2025**, *11*, 100560. [CrossRef]
22. FAO. *Assessment of Agricultural Plastics and Their Sustainability: A Call for Action*; FAO: Rome, Italy, 2021; ISBN 978-92-5-135402-5.
23. Hayes, D.G. Impact of Plastics in Agriculture. *Agriculture* **2025**, *15*, 322. [CrossRef]
24. Hofmann, T.; Ghoshal, S.; Tufenkji, N.; Adamowski, J.F.; Bayen, S.; Chen, Q.; Demokritou, P.; Flury, M.; Hüffer, T.; Ivleva, N.P.; et al. Plastics Can Be Used More Sustainably in Agriculture. *Commun. Earth Environ.* **2023**, *4*, 332. [CrossRef]
25. Ingram, J. A Food Systems Approach to Researching Food Security and Its Interactions with Global Environmental Change. *Food Secur.* **2011**, *3*, 417–431. [CrossRef]
26. Maraveas, C. The Sustainability of Plastic Nets in Agriculture. *Sustainability* **2020**, *12*, 3625. [CrossRef]
27. Pagnotta, L. Sustainable Netting Materials for Marine and Agricultural Applications: A Perspective on Polymeric and Composite Developments. *Polymers* **2025**, *17*, 1454. [CrossRef]
28. Pekgokgoz, R.K.; Yakut, I. Investigation of Passive Controlled Post-Tensioning System on the Structural Behaviour of Precast Reinforced Concrete Beam–Column Connections. *Buildings* **2024**, *14*, 3910. [CrossRef]
29. Kang, L.; Zhang, Y.; Kacira, M.; van Hooff, T. CFD Simulation of Air Distributions in a Small Multi-Layer Vertical Farm: Impact of Computational and Physical Parameters. *Biosyst. Eng.* **2024**, *243*, 148–174. [CrossRef]
30. Briassoulis, D.; Hiskakis, M.; Tserotas, P. Combined Effect of UVA Radiation and Agrochemicals on the Durability of Agricultural Multilayer Films. *Polym. Degrad. Stab.* **2018**, *154*, 261–275. [CrossRef]
31. Picuno, P.; Godosi, Z.; Picuno, C. Agrochemical Contamination and Ageing Effects on Greenhouse Plastic Film for Recycling. *Appl. Sci.* **2022**, *12*, 10149. [CrossRef]
32. Puglisi, R.; Cillis, G.; Statuto, D.; Picuno, P. Recycled Plastics Used in the Production of Agricultural Nets for Crop Protection. In *Proceedings of the AIIA 2022: Biosystems Engineering Towards the Green Deal*; Ferro, V., Giordano, G., Orlando, S., Vallone, M., Cascone, G., Porto, S.M.C., Eds.; Springer International Publishing: Cham, Switzerland, 2023; pp. 1203–1210.
33. Baeza, E.; Hemming, S.; Stanghellini, C. Materials with Switchable Radiometric Properties: Could They Become the Perfect Greenhouse Cover? *Biosyst. Eng.* **2020**, *193*, 157–173. [CrossRef]
34. Cohen, S.; Fuchs, M. Measuring and Predicting Radiometric Properties of Reflective Shade Nets and Thermal Screens. *J. Agric. Eng. Res.* **1999**, *73*, 245–255. [CrossRef]
35. Andrady, A.L.; Barnes, P.W.; Bornman, J.F.; Gouin, T.; Madronich, S.; White, C.C.; Zepp, R.G.; Jansen, M.A.K. Oxidation and Fragmentation of Plastics in a Changing Environment; from UV-Radiation to Biological Degradation. *Sci. Total Environ.* **2022**, *851*, 158022. [CrossRef]
36. Martellotta, A.M.N.; Blanco, I.; Castellano, S.; Mastronardi, G.; Picuno, P.; Starace, G.; Puglisi, R.; Mugnozza, G.S. Rainwater Permeability of Agricultural Nets Under Different Installation Conditions as a Function of Rainfall Intensity. *Agriculture* **2026**, *16*, 340. [CrossRef]
37. *UNI 9405:1989*; Determinazione della Forza e dell'Allungamento a Rottura. UNI Ente Italiano Di Normazione: Milano, Italy, 1989.
38. *UNI EN ISO 13934-1:2013*; Tessili—Proprietà dei Tessuti a Trazione—Parte 1: Determinazione della Forza Massima e dell'Allungamento alla Forza Massima con il Metodo della Striscia. UNI Ente Italiano Di Normazione: Milano, Italy, 2013.
39. Tucman, I.; Pilipović, A. The Effect of Ageing on the Tensile Properties of Greenhouses Nets. *Eur. Mech. Sci.* **2024**, *8*, 210–217. [CrossRef]
40. Picuno, P.; Tortora, A.; Sica, C. Mechanical Characterization of Plastic Nets for Protected Cultivation. *Acta Hortic.* **2008**, *801*, 91–98. [CrossRef]